Leptonic decay widths of the ϕ-meson

M. Antonelli and M. Dreucci
Laboratori Nazionali di Frascati

July 26, 2004

Abstract

The ϕ-meson leptonic widths, Γ_{ee} and $\Gamma_{\mu\mu}$, are obtained from the e^+e^- forward-backward asymmetry and the $\mu^+\mu^-$ cross section around the ϕ-mass energy. We find Γ_{ee}=1.32±0.05±0.03 keV and $\sqrt{\Gamma_{ee}\Gamma_{\mu\mu}}$=1.320±0.018±0.017 keV. These results, compatible with $\Gamma_{ee}=\Gamma_{\mu\mu}$, provide a most precise test of lepton universality. Combining the two results gives $\Gamma_{\ell\ell}(\phi) = 1.320 \pm 0.023$ keV.

1 Introduction

The ϕ-leptonic widths provide information on the ϕ-structure and the production cross section in e^+e^-annihilations. They are necessary for decay branching ratio measurements and estimates of the hadronic contribution to vacuum polarization [1, 2]. The lowest order amplitudes for $e^+e^- \to e^+e^-$, $\mu^+\mu^-$ are shown in Fig. 1. The total cross sections can be

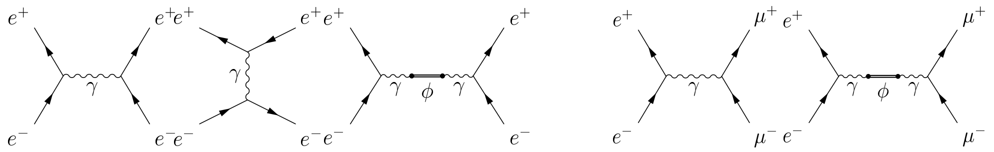

Figure 1: Amplitude for $e^+e^- \to e^+e^-$, left and $e^+e^- \to \mu^+\mu^-$, right, at $W \sim M(\phi)$

written as $\sigma_{ee} = \sigma_{ee,\phi} + \sigma_{\rm int}$ and $\sigma_{\mu\mu} = \sigma_{\mu\mu,\phi} + \sigma_{\rm int}$. The interference term:

$$\sigma_{\rm int} = \frac{3\alpha\Gamma_{\ell\ell}}{M_\phi} \frac{s - M_\phi^2}{(s - M_\phi^2)^2 + s\Gamma_\phi^2} \int_{\cos\theta_-}^{\cos\theta_+} {\rm d}\cos\theta f(\theta)_{\ell\ell} \tag{1}$$

is linear in $\Gamma_{\ell\ell}$, where $\Gamma_{\ell\ell} = \Gamma_{ee}$ for $e^+e^-\to e^+e^-$ and $\Gamma_{\ell\ell} = \sqrt{\Gamma_{ee}\Gamma_{\mu\mu}}$ for $e^+e^- \to \mu^+\mu^-$. σ_{int} changes sign when s goes through M_ϕ^2. The angular distributions for e^+e^- and $\mu^+\mu^-$ are, respectively:

$$f(\theta)_{ee} = 2\left[1 + \cos^2\theta - \frac{(1+\cos\theta)^2}{1-\cos\theta}\right]$$

$$f(\theta)_{\mu\mu} = \beta_\mu\left[1 + \cos^2\theta + (1-\beta_\mu^2)\sin^2\theta\right]$$

with β_μ the muon velocity. In the following we use data collected at center of mass, CM, energies W of 1017.2 and 1022.2 MeV, i.e. $M_\phi \pm \Gamma_\phi/2$, as well as the large sample collected W=1019.7 MeV. For $e^+e^- \to \mu^+\mu^-$ we measure the cross section. Since Bhabha scattering is dominated by the photon exchange amplitude, the interference term is best studied in the forward-backward asymmetry, A_{FB}, defined as

$$A_{FB} = \frac{\sigma_F - \sigma_B}{\sigma_F + \sigma_B}. \tag{2}$$

where σ_F and σ_B are the cross sections for events with electrons in the forward and backward hemispheres. Fig. 2 shows A_{FB} and $\sigma_{\mu\mu}$ vs W for $\Gamma_{\ell\ell}$=1.2, 1.3 and 1.4 keV keV. A fractional change of 3% in $\Gamma_{\ell\ell}$ (the present accuracy on $\Gamma_{\mu\mu}$ [3]) results in a fractional change of $\sim 3 \times 10^{-4}$ and $\sim 4 \times 10^{-3}$ for A_{FB} and $\sigma_{\mu\mu}$. Radiative corrections for initial

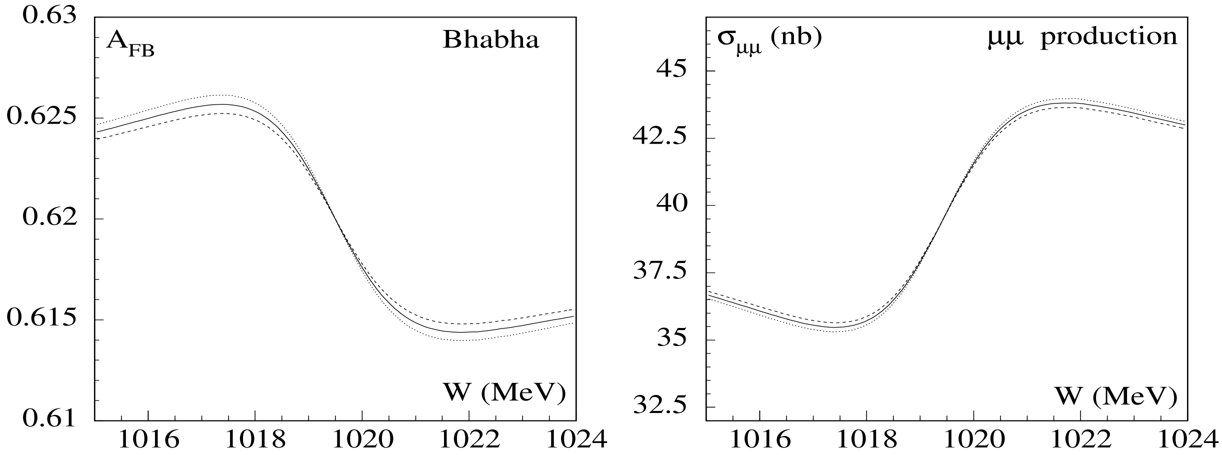

Figure 2: Left: A_{FB} sensitivity to $\Gamma_{\ell\ell}$. Right: $\sigma_{\mu\mu}$ sensitivity to $\Gamma_{\ell\ell}$. See text.

state radiation (ISR) and final state radiation (FSR) are included following [4, 5]. Initial state radiation, where one or both the initial colliding particles radiate a photon before interacting, changes the collision energy. ISR photons are mostly collinear to the beam, and therefore not detectable. The effective center-of-mass energy is reduced from the nominal value, W, to a lower value, W'. FSR, by interference with ISR, introduces an asymmetry in the angle distribution. To enhance the ϕ-meson contribution, a lower cut on W'/W is imposed for both $e^+e^- \to e^+e^-$ and $e^+e^- \to \mu^+\mu^-$ processes. We define the variable:

$$z = \sqrt{\frac{\sin\theta_+ + \sin\theta_- - |\sin(\theta_+ + \theta_-)|}{\sin\theta_+ + \sin\theta_- + |\sin(\theta_+ + \theta_-)|}} \tag{3}$$

where θ_+ and θ_- are the angles of the final positive and negative leptons, in the nominal collision CM. For a single collinear ISR photon and collinear FSR photons, we have $W'/W = z$. If an event contains two or more ISR photons then, unless these photons all go in the same direction, equation $W'/W = z$ is no more exact. In the collision CM, because of ISR, final particles are not back to back. To define our geometrical acceptance we use the polar angle in the frame of the final leptons. In the following we refer to the polar angle θ as the average of the θ_- and $180° - \theta_+$ in this frame.

2 Detector and Data Sample

The KLOE detector consist of an electromagnetic calorimeter, ECAL and a large drift chamber, DC. The calorimeter, consisting of a barrel covering $45° < \theta < 135°$ and two end caps, measures energy with a resolution $\sigma(E)/E = 5.7\%/\sqrt{E(\mathrm{GeV})}$ and arrival times with a resolution $\sigma(t) = [54/\sqrt{E(\mathrm{GeV})} \oplus 50]$ ps. All triggers are reconstructed quasi on line and stored in a tape library. Luminosity, $\mathcal{L}$ and accelerator parameters, energy, etc., are obtained from Bhabha scattering. The luminosity has an energy independent systematic uncertainty of 0.6%. The absolute energy scale is fixed using to the CMD-2 ϕ-meson mass: $m(\phi) = 1019.48 \pm 0.01 \pm 0.03$ [6]. The CM energies and $\int \mathcal{L} dt$ for the collected data are summarized in Table 1. Analysis efficiencies, acceptance cuts, background and

CM energy (MeV)	$\int Ldt$ (nb^{-1})
1017.17 ± 0.01	6966 ± 42
1019.72 ± 0.02	4533 ± 27
1022.17 ± 0.01	5912 ± 35

Table 1: 2002 ϕ-scan statistics

the resolution in θ are determined with the help of GEANFI [7], the KLOE Monte Carlo (MC) program. GEANFI uses the Babayaga generator [8] to account for ISR effects. FSR corrections are evaluated with a Novosibirsk [9] MC program. For the study of $e^+e^-\to\mu^+\mu^-$ we have developed an additional MC code, appropriately including ISR and FSR.

3 Γ_{ee} measurement from Bhabha events

3.1 Analysis

Bhabha events are selected using ECAL and DC information. We only use events for which the polar angle satisfies $53° < \theta < 127°$, corresponding to the central region of the barrel calorimeter. Muon and pion contamination is quite negligible. For each event we evaluate $z_{\mathrm{m}} = z$ defined in eq. 3, and retain events with $z_{\mathrm{m}} > 0.95$. Fig. 3 and 4 show the distribution of z_{m} for the signal ($W'/W > 0.95$) and the radiative background ($W'/W < 0.95$), obtained with Geanfi Monte Carlo. The efficiency and the radiative background have been evaluated as a function of the polar angle. On average, an efficiency of about 98% and a contamination of radiative bachground of about 2% are obtained for $x_{\mathrm{m}} > 0.95$. In this analysis some of the systematics are independent of W and

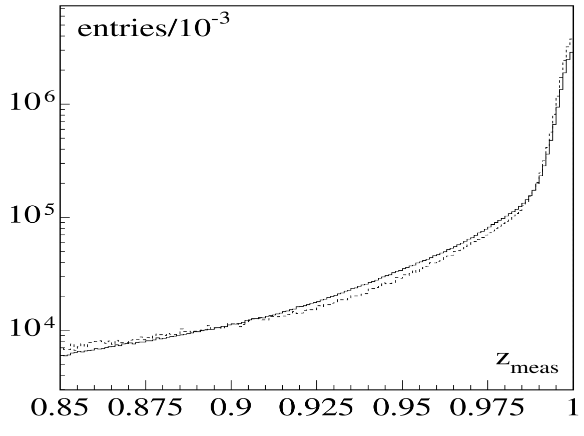

Figure 3: $e^+e^- \to e^+e^-$. z_{m} distribution for data (solid) and MC (dot)

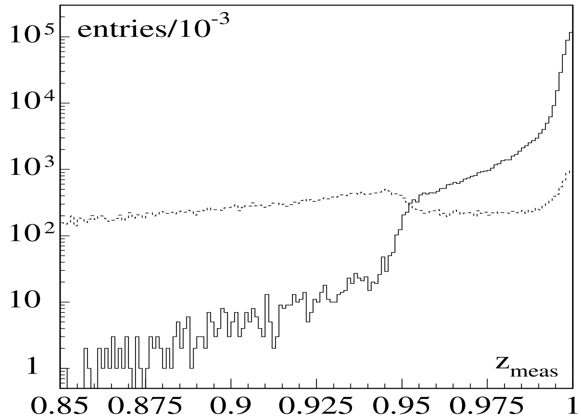

Figure 4: $z_{\rm m}$ for $e^+e^- \to e^+e^-$ MC events: signal ($W'/W > 0.95$, solid) and radiative background ($W'/W < 0.95$, dot)

do not affect the measurement of Γ_{ee}: they amount to 0.2% and are dominated by the uncertainty on FSR correction (see next section) and by the θ resolution. The θ resolution is ∼3 mrad, from the MC simulation. The finite resolution introduces no bias but reduces the asymmetry. We find the reduction to be 0.0011 ± 0.0004. Systematic errors on A_{FB} due to $z_{\rm m}$ resolution, θ cut and background are evaluated by varying the acceptance cuts. They are summarized in Table 2.

Fiducial cuts	W=1017.17	W=1019.72	W=1022.17
$0.90 < z_{\rm m} < 0.98$	0.00008	0.00003	0.00011
$50° < \theta < 70°$	0.00010	0.00010	0.00010

Table 2: Systematic uncertainties on A_{FB}

3.2 Results

Table 3 shows the asymmetry for $z_{\rm m} > 0.95$ and $53° < \theta < 127°$, together with the errors. The common systematic error of 0.2% mentioned before is not included. To

W (MeV)	A_{FB}
1017.17	0.6275 ± 0.0003
1019.72	0.6205 ± 0.0003
1022.17	0.6161 ± 0.0004

Table 3: Forward-backward asymmetry results for $z_{\rm m} > 0.95$ and $53° < \theta < 127°$

fit these results we first convolute the cross section with the radiator function [4, 5] in order to account for ISR. We then fold-in the machine energy spread (BES), ∼330 keV in the center-of-mass energy [10]. The FSR correction is negligible, ∼ 0.02%, as evaluated from the Novosibirsk MC code, giving an uncertainty of 0.15% on A_{FB}. The ω-exchange contribution is expected to be very small, because $m_\phi - m_\omega \sim 29 \times \Gamma_\omega$. In fact, its inclusion in the amplitude indicates that the systematic error on Γ_{ee} is less than 0.1%. The fit parameters are the leptonic width, Γ_{ee}, the ϕ mass, M_ϕ, and the forward-backward asymmetry at the ϕ mass, A^0 . The ϕ width is taken from PDG [11], $\Gamma_\phi = 4.26 \pm 0.05$ MeV. Its uncertainty results in an uncertainty of 0.013 keV for Γ_{ee}. The difference between

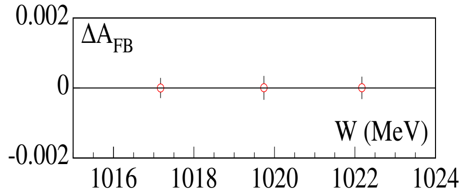

Figure 5: Difference between fit values and data for A in $e^+e^- \to e^+e^-$.

fit values and data is shown in Fig. 5. The error on M_ϕ stems from the determination of W, $\sim$30 keV [11]. The results of the fit to the data are shown in Table 4. Note that the asymmetry measurement does not depend on luminosity, trigger efficiency and acceptance.

Parameter	value	stat.error	syst.error
Γ_{ee} (keV)	1.32	0.05	0.03
A^0 (deg)	0.6215	0.0002	0.002
M_ϕ (MeV)	1019.50	0.08	0.03

Table 4: Fit results for $e^+e^- \to e^+e^-$ process

4 $\sqrt{\Gamma_{ee}\Gamma_{\mu\mu}}$ from $ee \to \mu\mu$

4.1 Analysis

Selection of $e^+e^- \to \mu^+\mu^-$ events is based on the fact that muons have lower response in the EM calorimeter. We require two tracks with $970 < |\vec{p}_+|+|\vec{p}_-| < 1010$ MeV and a total energy deposited in the electromagnetic calorimeter less than 700 Mev, Fig. 6. Background is due to $ee \to \pi\pi$ events, see later. In order to reduce systematic uncertainties from the the cut on the sum of momentum magnitudes, a tighter cut on the invariant mass, $M_{\pi\pi} \sim (W-20)$ MeV, has been applied. We also require $50° < \theta < 130°$. The angular distribution is distorted with respect to $1+\cos^2\theta$, because of ISR-FSR interference, as shown in Fig. 7. Similarly to the $e^+e^- \to e^+e^-$ case, we require $z_\mathrm{m} > 0.985$. This choice is determined by a preliminary cut imposed at the online reconstruction. The distribution of z_m for data and MC is shown in Fig. 8. The efficiency loss below 0.98 is clearly visible, is due to a cut on the sum of the magnitudes of the particle momenta. A corresponding disagreement between data and MC is due to missing NLO-FSR effects in the generator. θ and z_m are computed as for $e^+e^- \to e^+e^-$ events.

4.2 Experimental data and results

Muon (signal) and pion (background) counting is obtained from fitting the two particles invariant mass distribution, for each collider energy. The mass distribution for $\pi^+\pi^-$ and $\mu^+\mu^-$ is obtained from an additional MC code, which includes ISR and FSR, and in which mass resolution and machine energy spread have been folded in. A fit example is shown in Fig. 9. The mass resolution is obtained from data. If E_+ and E_- are the final particle energies in the collision frame, $E_+ + E_-$ is the invariant mass. The variance of the energy sum is equal to that of the difference $E_+ - E_-$, which is trivially obtained from data.

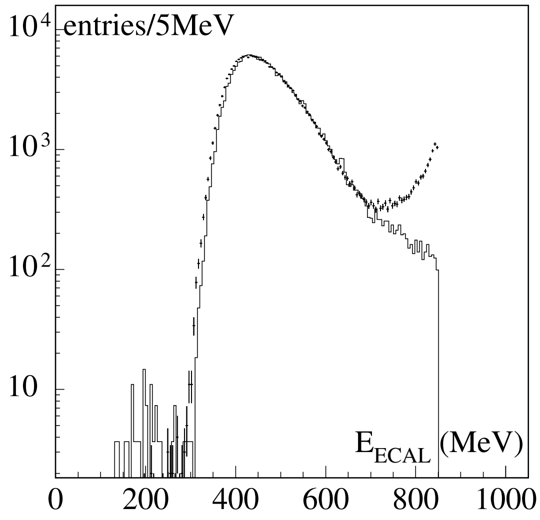

Figure 6: Total energy in the electromagnetic calorimeter for MC, histogram, and data. The Bhabha contamination is visible.

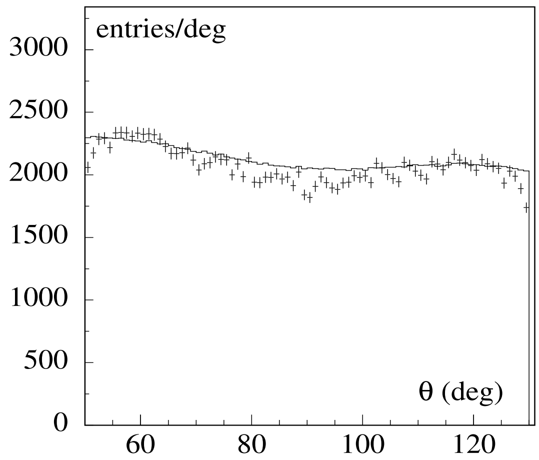

Figure 7: θ distribution. Data and Novosibirsk MC simulation are in agreement. Deviation from $1 + \cos^2\theta$ is due to ISR-FSR interference.

Note that BES contributions cancel out. Also ISR and FSR, as a first approximation, cancel out. Some efficiencies are evaluated using GEANFI MC (acceptance cuts, 700 MeV calorimeter energy cut, tracking efficiency). The efficiencies due to the trigger and off line filter algorithms have been evaluated directly from data, by reprocessing raw data from a single run. All of these uncertainties are identical at all energies. They affect the cross-section measurement but not $\Gamma_{\ell\ell}$. All contributions are shown in Table 5. These contributions, together with the uncertainty of the luminosity (0.6%) produce a common systematic error of 1.2% on $\sigma_{\mu\mu}$. The systematic errors due to the signal ($ee \to \mu\mu$) and background ($ee \to \pi\pi$) counting derive basically from the invariant mass experimental resolution, and amount to about 0.0045 nb. The errors due to the acceptance cuts on z_m and θ result to be 0.01 nb, and 0.002 nb, respectively. The Bhabha contamination contribution is negligible, $\ll 0.2\%$. Table 6 gives the cross section for $e^+e^- \to \mu^+\mu^-$. To fit the data, the cross section is corrected for ISR and convoluted with the machine energy spread. Free parameters are the leptonic width, $\Gamma_{\ell\ell} = \sqrt{\Gamma_{ee}\Gamma_{\mu\mu}}$, the ϕ mass, M_ϕ, and the cross section at the ϕ mass, σ_0. The result of this fit is shown in Fig. 10. The ϕ

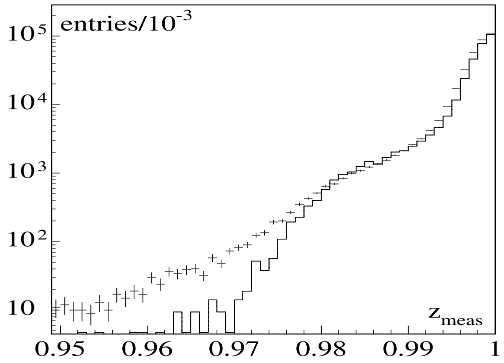

Figure 8: $z_{\rm m}$ distribution for MC, histogram, and data.

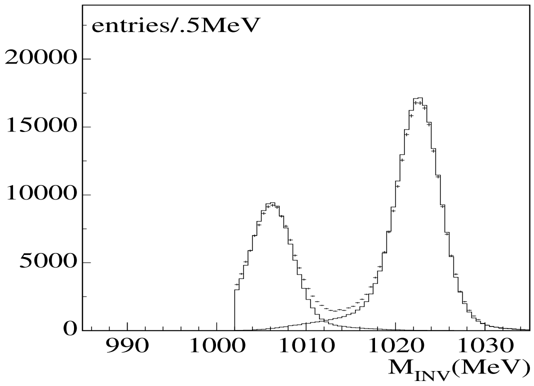

Figure 9: Fit to the mass distribution of $\pi^+\pi^-$ and $\mu^+\mu^-$ events for W=1022 MeV.

width uncertainty gives an error of 0.013 keV keV on $\Gamma_{\ell\ell}$. The ω exchange contribution is negligible. The FSR correction, evaluated by MC simulation, produces a 0.004 keV error $\Gamma_{\ell\ell}$. The results are summarized in Table 7.

5 Conclusion

Our results, $\Gamma_{ee} = 1.32 \pm 0.05 \pm 0.03$ keV and $\sqrt{\Gamma_{ee}\Gamma_{\mu\mu}} = 1.320 \pm 0.018 \pm 0.017$ keV, are consistent with lepton universality within our errors. Combining the two results we find for the leptonic width of the ϕ-meson $\Gamma_{\ell\ell} = 1.320 \pm 0.017 \pm 0.015$ keV, with a total uncertainty of less than 2%.

References

[1] S. Eidelman, F. Jegerlehner. *Z.Phys.* **C67** (1995), 585.

[2] C. Quigg, J.L. Rosner. *Z.Phys.* **C67** (1995), 585; H. Gross, A. Martin *Phys.Rept.***60** (1980), 341; R. Van Royen; V.F. Weisskopf; *Nuovo Cimento* **A50** (1967), 617 and err. ibid. **A51**; E.C. Poggio, H.J. Schnitzer *Phys.Rev.* **D20** (1979), 1175 and err. ibid. **D21**; H. Krasemann *Phys.Lett.* **B96** (1980), 397; T.D. Newton, E.P. Wigner *Rev.Mod.Phys.* **21** (1949), 400.

[3] M.N. Achasov et al.; *Direct measurement of the ϕ(1020) leptonic branching ratio. Budker INP 2000-71, preprint*

source	relative contribution
Trigger + offline	$7 \cdot 10^{-3}$
Tracking	$5 \cdot 10^{-3}$
ECAL cut	$5 \cdot 10^{-3}$
Total	0.01

Table 5: Common $\sigma_{\mu\mu}$ systematic errors.

CM energy (MeV)	$\sigma_{\mu\mu}$(nb)
1017.17	35.66 ± 0.08
1019.72	40.19 ± 0.14
1022.17	43.92 ± 0.09

Table 6: Cross-section $ee \to \mu\mu$. Common errors on $\sigma_{\mu\mu}$ are not included

Parameter	value	stat.error	syst.error
$\Gamma_{\ell\ell}$ (keV)	1.320	0.018	0.016
M_ϕ (MeV)	1019.63	0.04	0.03
σ_0 (nb)	39.2	0.04	0.4

Table 7: Fit results for $e^+e^- \to \mu^+\mu^-$ process.

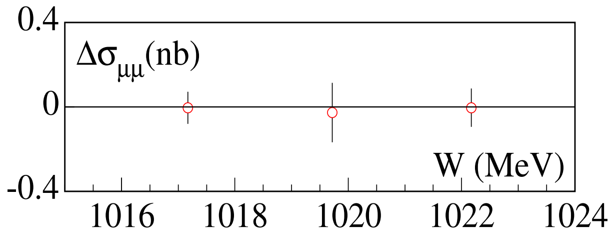

Figure 10: Fit result for $e^+e^- \to \mu^+\mu^-$ process.

[4] M. Greco, G. Montagna, O. Nicosini, F. Piccinini. QED radiative corrections and radiative Bhabha scattering at DaΦne *"The second DAϕNE physics handbook"*, 629.

[5] E.A. Kuraev, V.S. Fadin. *On radiative corrections to the cross section for single-photon annihilation of an e+e- pair at high energy* Sov.J.Phys. **41** (1985), 466.

[6] R.R. Akhmetshin et al.; Phys.Lett. **B466** (1999), 385.

[7] A. Antonelli, C. Bloise; *The Kloe Monte Carlo GEANFI* Kloe memo **128**.

[8] C.M. Carloni Calame et al.; Nucl.Phys. **B584** (2000), 459.

[9] A. Sibidanov; private comunication.

[10] C. Gatti, T. Spadaro; *Kloe Memo in preparation.*

[11] Review of Particle Physics, Phys.Lett. **B592**, 1 (2004)